ORIGINAL PAPER

Drought history and vegetation response in the Angolan Highlands

Mauro Lourenco[1,2] · Stephan Woodborne[1,3] · Jennifer M. Fitchett[1]

Abstract

Drought negatively impacts health systems, agriculture, economies, energy, and the natural environment. The vulnerability of the Angolan Highlands rural communities that are dependent on rain-fed agriculture is a concern due to the prospect of climate change and the trajectory of increasing frequency of droughts in the region. The Angolan Highlands is an essential source water region for the Okavango Delta, and southern Africa more broadly. This study integrates Climate Hazards Group InfraRed Precipitation with Station data (CHIRPS) and vegetation indices from moderate resolution imaging spectroradiometer (MODIS) in the first historical assessment of drought in the Angolan Highlands. Using the standardized precipitation index (SPI), eight distinct drought periods were identified: 1981–1982, 1989–1990, 1994, 1995–1997, 1999–2000, 2014–2016, 2017–2018, and 2018–2020, with the frequency of drought increasing since 1981. The relationship between drought occurrence and El Niño Southern Oscillation (ENSO) is not linear; with two of the eight drought periods occurred exclusively during El Niño years. The seasonality of precipitation, MODIS enhanced vegetation index (EVI), and normalized difference vegetation index (NDVI) are similar, with NDVI and EVI being lowest at the end of the dry winter months (August), and highest during the summer rainfall season. The strong relationship between precipitation and vegetation, anthropogenic pressure on the landscape, and increased drought occurrence are likely to lead to potential environmental degradation in future. Mitigation and adaptation strategies to drought may be required, especially concerning water resources and agricultural practices within the Angolan Highlands region.

1 Introduction

Drought is a persistent natural hazard and is one of the most damaging to health (Ebi and Bowen 2016), agriculture (Nath et al. 2017), economies (Ahmadalipour et al. 2019), and the natural environment (Bachmair et al. 2016). The World Health Organisation (WHO 2021) estimates that this phenomenon affects 55 million people globally each year, leading to famine, water shortages, migration, disease, and death (Ebi and Bowen 2016; Luetkemeier and Liehr 2019). Between 1900 and 2013, it is estimated that approximately 850,000 people died, and more than 350 million people were affected by drought events in Africa (Ahmadalipour et al. 2019; Luetkemeier and Liehr 2019). Across sub-Saharan Africa, major droughts occurred in the early 1970s, mid 1980s and early 1990s (Luetkemeier and Liehr 2019). Drought occurrence is intensifying in frequency and severity in southern Africa, presenting challenges to long-term water and food security in the region (Nhamo et al. 2019; Gore et al. 2020).

Angola experienced severe drought events in the early 1990s and 2000s (Rouault and Richard 2005) as well as a perennial drought from 2013 to 2016, and again in 2019 (Regional Vulnerability Assessment and Analysis Programme: RVAA 2019) which have been linked to the El Niño Southern Oscillation (ENSO; Luetkemeier and Liehr 2019; Gore et al. 2020). Angola also experienced drought during 2020/2021, when cumulative rainfall was 30% below the long-term average (Food and Agriculture Organisation of the United Nations: FAO 2021). The Angolan people are vulnerable during prolonged drought periods: A total of 11.1 million people (37%) of the population live in rural regions (RVAA 2019), and the majority of them practice rain-fed subsistence agriculture (Luetkemeier and Liehr 2019).

✉ Jennifer M. Fitchett
  Jennifer.Fitchett@wits.ac.za

1   School of Geography, Archaeology and Environmental Studies, University of the Witwatersrand, Johannesburg, South Africa

2   National Geographic Okavango Wilderness Project, Wild Bird Trust, Hogsback, South Africa

3   iThemba LABS, Private Bag 11, WITS, Johannesburg, South Africa

Retrospective analysis of precipitation data is extremely valuable in determining the severity of past drought events, aiding in response development and mitigation strategies (Mishra and Singh 2010; Mlenga et al. 2019). The dependence of the Angolan population on hydroclimatic conditions underscores the importance of accurate assessment of past drought occurrence and drought monitoring for potential disaster management in future.

Traditional definitions consider drought to be an extreme precipitation deficit (González and Valdés 2006; AghaKouchak et al. 2021) in a specific region that persists for a defined period of time (Zargar et al. 2011). Physical drought types include meteorological, agricultural, and hydrological drought (Zargar et al. 2011). Additional drought types, which have received increased attention, include anthropogenic, socioeconomic, and ecological drought (Kchouk et al. 2022), with a new focus on drought being defined as a process and not a product (AghaKouchak et al. 2021). In addition to drought type, droughts are also characterized by severity, duration, spatial distribution, frequency, magnitude (cumulated deficit), predictability, rate of onset, and timing (Mishra and Singh 2010; Zargar et al. 2011). Determining drought onset, duration, and termination is complex, presenting difficulties in accurate and effective drought monitoring (Mishra and Singh 2010; Mlenga et al. 2019).

Over 100 different drought indices have been proposed, many of which are functions of precipitation with or without temperature, and with or without river discharge (Zargar et al. 2011). Common drought indices include the standardized precipitation index (SPI: McKee et al. 1993), percent of normal, Palmer drought severity index (PDSI: Palmer 1965), the standardized precipitation evaporation index (SPEI: Vicente-Serrano et al. 2010), Deciles (Gibbs and Maher 1967), crop moisture index (CMI: Palmer 1968), and reconnaissance drought index (RDI: Tsakiris and Vangelis 2005). The SPI is a widely used meteorological drought index that is simplified so that it only depends on precipitation data, resulting in a single numeric value (McKee et al. 1993; Komuscu 1999). In 2009, the World Meteorological Organisation (WMO) Lincoln Declaration recommended SPI as the primary meteorological drought index (Svoboda et al. 2012). This is because SPI allows the comparison between different climates and locations and can be used to monitor dry or wet periods for any location with regular precipitation data (McKee et al. 1993; Moreira et al. 2008). The index can be computed for multiple time periods, reflecting precipitation deficits of different water resources and can identify various drought types (Svoboda et al. 2012).

Reliance on meteorological data alone may be inadequate in monitoring drought across all regions, especially in southern Africa where data is likely to be incomplete, unreliable, unavailable, and untimely (Mlenga et al. 2019). In such situations, satellite imagery may be used to assess the spatial and temporal dimensions of drought. Satellite data can be used to obtain a better understanding of the pressures on water resources, vegetation, and society to drought (Didan 2015; Gao et al. 2020). The normalized difference vegetation index (NDVI) and enhanced vegetation index (EVI) are widely used drought indices obtained from satellite data (Didan 2015; Liou and Mulualem 2019; Gao et al. 2020). Both NDVI and EVI have been used for estimation of vegetation health, coverage, net primary production, crop growth conditions, yield assessments and estimation, vegetation type, phenology, and land cover changes, and contribute to drought monitoring and early warning systems (Brown et al. 2008; Liou and Mulualem 2019; Hua et al. 2019). Vegetation which is particularly vulnerable to drought can be studied for drought risk management and can be used to map areas affected by drought (Alamdarloo et al. 2018; Liou and Mulualem 2019).

The Angolan Highlands is the water source region for three major river catchments in sub-Saharan Africa, including the Congo River to the North, the Zambezi River to the East, and the Okavango system to the south (Lourenco et al. 2022). The Angolan Highlands support transboundary rivers that flow from Angola to Namibia, Botswana, Zambia, the Democratic Republic of the Congo, Mozambique, and Zimbabwe. The highlands are the only source region of the Okavango Delta, a UNESCO world heritage site (Marazzi et al. 2017; Yurco et al. 2017; UNESCO 2021). Civil war between 1975 and 2002 and persistent minefields have hampered access to the region, and despite its hydrological and ecological significance, it is little studied (Carvalho et al. 2017; Lourenco et al. 2022). Climate variability in the region is one of the strongest drivers of rainfall variability over a subcontinent that is largely dependent on rain-fed agriculture (Crétat et al. 2019; Huntley et al. 2019). Despite its importance, there are no studies, specific to this region that might explain the variability and history of drought, the potential vegetation response and consequences on local communities. This study integrates Climate Hazards Group InfraRed Precipitation with Station data (CHIRPS) and the SPI with NDVI and EVI for historical assessment of drought monitoring in the southeast of the Angolan Highlands.

2 Methods

2.1 Study area

The Angolan Highlands study site is in the southeast of Angola, spanning a latitudinal range 11°54′-13°54′S and longitudinal range 18°05′-20°34′E, and covering approximately 61,590 km^2 (Fig. 1). It is part of an extensive interior plateau, characterized by a vast peneplain of Kalahari sand (Goyder et al. 2018; Huntley et al. 2019). The climate is
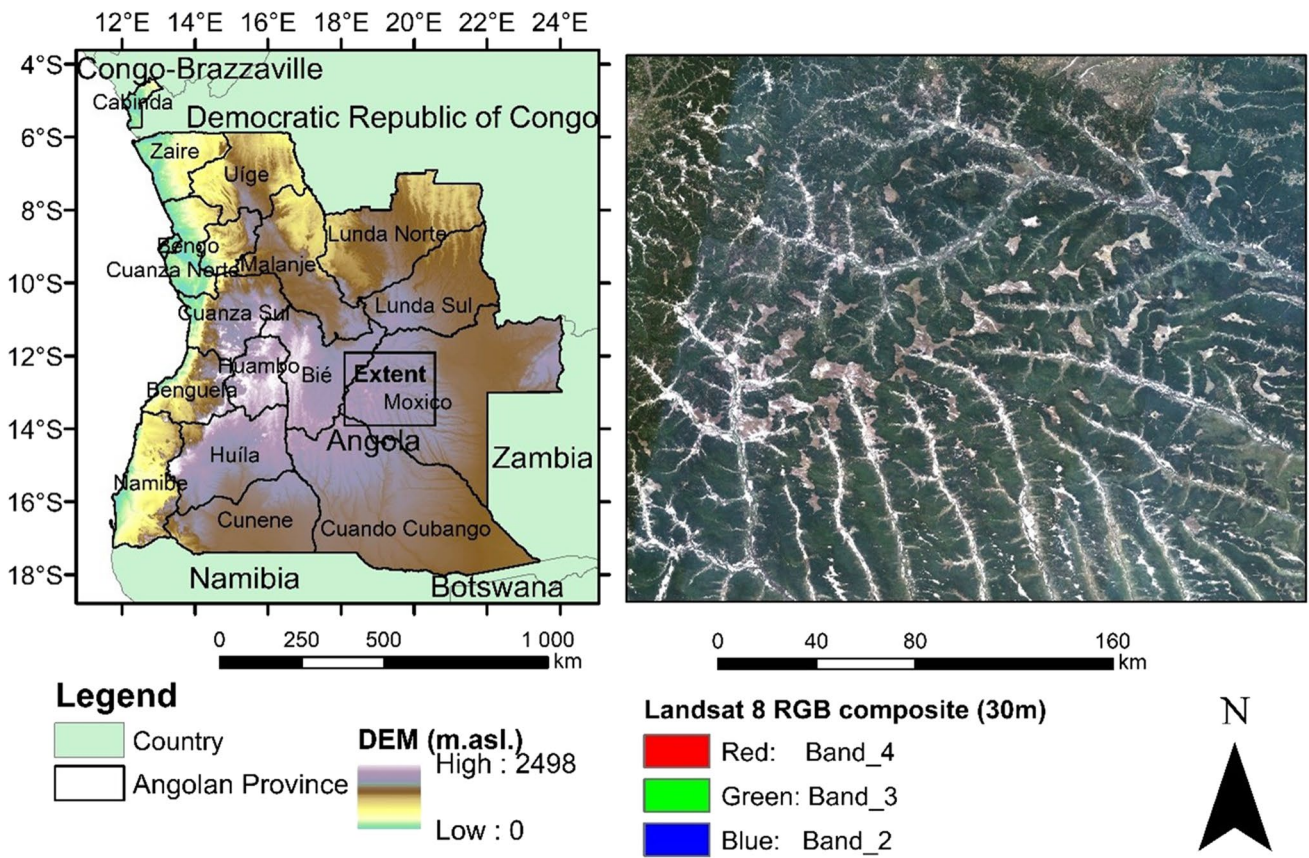
Fig. 1 Study area map showing the study site extent in Angola and a Landsat 8 (USGS, 2021) red, green blue (RGB) optical image of the study site

strongly seasonal, with hot, wet summers from October to May and mild to cool, dry winters from June to September (Abiodun et al. 2019; Huntley et al. 2019). The highlands lie within the Angolan miombo woodland ecoregion and contain tropical and subtropical grasslands, tree, and shrub savannas (Goyder et al. 2018; Huntley et al. 2019). The wide river valleys are characterized by extensive wet grasslands, peatlands, and ox-box lakes and the surrounding hills are dominated by miombo woodland (Conradie et al. 2016; Goyder et al. 2018; Lourenco et al. 2022).

2.2 Precipitation data

Studies of the climate of Angola have been hindered over the past four decades due to the collapse of the extensive network of weather stations during the civil war, and the resultant poor national coverage of meteorological data, and lack of reliability of climatic data collected (Huntley et al. 2019). The weather recording network reduced from 225 climatological stations in 1974 to zero in 2010, while the number of actively recording synoptic stations decreased from 29 in 1974 to 23 operational stations in 2010, of which 12 are automatic and 11 conventional

(Huntley et al. 2019). Since 2010, the network has been strengthened by 22 automatic stations established by the Southern African Science Service Centre for Climate Change and Adaptive Land Management (SASSCAL, Huntley et al. 2019). A minimum of 30 years of continuous precipitation data are needed for reliable calculations of the SPI, and even longer archives are favourable (McKee et al. 1993). The precipitation data for the study has been collected from a remote sensing product, as historical climate data from weather stations, specific to this study area, are unavailable.

Historical precipitation data for the region were collated using the Google Earth Engine (GEE) platform. Precipitation data were obtained from the CHIRPS 30 + year quasi-global rainfall dataset (Funk et al. 2015). CHIRPS synthesises 0.05° resolution satellite imagery with in-situ station data to create gridded rainfall time series for trend analysis and seasonal drought monitoring (Funk et al. 2015). On GEE, daily precipitation data was collated for the period spanning 40 years from 1981–01-01 to 2020–12-31. The daily precipitation values represent the mean of all pixels over the delineated study area of interest at 5 km resolution. This data was used to create both a time-series of daily precipitation over the period

of interest, and to produce maps of the spatial distribution of precipitation over the region using ArcMap 10.2.

2.3 Standardized precipitation index

The SPI was calculated using the methods described by McKee et al. (1993). The SPI generator v.1.7.5 was used following the procedure specified in the WMO SPI User Guide (Svoboda et al. 2012). The SPI was calculated using the CHIRPS daily precipitation data which had no missing values over the full historic archive. The SPI calculation for any location is based on the long-term precipitation record for a period of interest. The SPI can be computed for multiple periods, but is commonly applied for 1-, 3-, 6-, 12-, 24-, 36-, and 48-month periods (Svoboda et al. 2012; Tirivarombo et al. 2018; Mlenga et al. 2019). Meteorological and soil moisture conditions (agriculture) respond to precipitation anomalies on relatively short timescales (1–6 months), whereas streamflow, reservoirs, and groundwater respond to longer-term precipitation anomalies from 6 months and up to 24 months or longer (Guttman 1999). SPI calculations shorter than 1 month or longer than 24 months may be unreliable, and statistically, 3–24 months is the best practical range of application (Guttman, 1999). Positive SPI scores indicate a greater than median precipitation, and negative scores indicate less than median precipitation (Svoboda et al., 2012). As the SPI is normalized, both wet and dry periods can be determined. Drought is defined in instances when scores are below − 1 (Table 1), and a drought is classified as having ended when SPI scores are positive (Edwards and McKee 1997).

2.4 EVI and NDVI data

The moderate resolution imaging spectroradiometer (MODIS) MOD13Q1.006 Terra Vegetation Indices 16-Day Global (Dida 2015) were used to calculate the NDVI and EVI for the time-period spanning 2000–02-18 to 2020–12-31. The MOD13Q1 V6 product provides a vegetation index value on a per pixel basis which in this dataset has 250 m resolution (Didan 2015). The NDVI is a normalized transform of the near infrared (NIR) to red reflectance ratio, designed to standardise vegetation index

values between -1 and + 1 (Dindan et al. 2015). Negative values indicate water, and low NDVI values (0.1 or less) indicate barren rock or sand. Sparse vegetation such as shrubs and grasslands is likely to result in moderate NDVI values between 0.2 and 0.5 and dense vegetation such as forests is likely to result high NDVI values between 0.6 and 0.9 (Didan 2015). It is commonly expressed as:

$$NDVI = \frac{NIR - Red}{NIR + Red} \tag{1}$$

(Rouse et al. 1974).

EVI is also standardized, having values between − 1 and + 1 and is similar to NDVI in that it can be used to quantify vegetation greenness. The EVI makes use of the blue and red band reflectances, which makes the index less vulnerable to aerosol contamination. In general, the scattering cross section in the blue band is larger than that in the red (Didan et al. 2015). When aerosol concentration is higher, the difference between the bands becomes larger. The EVI incorporates this atmospheric resistance, and in addition, EVI decouples the soil and atmospheric influences from the vegetation signal by including a feedback term for simultaneous correction (Didan et al. 2015). The EVI formula is:

$$EVI = G\frac{NIR - Red}{NIR + C1Red - C2Blue + L} \tag{2}$$

(Didan et al. 2015).

where NIR, Red, and Blue are the full or partially atmospheric-corrected (for Rayleigh scattering and ozone absorption) surface reflectance; L is the canopy background adjustment for correcting the nonlinear, differential NIR and red radiant transfer through a canopy; C1 and C2 are the coefficients of the aerosol resistance term (which uses the blue band to correct for aerosol influences in the red band); and G is a gain or scaling factor. The coefficients adopted for the MODIS EVI algorithm are L = 1, C1 = 6, C2 = 7.5, and G = 2.5 (Didan et al., 2015).

EVI minimizes canopy background variations and maintains sensitivity over dense vegetation conditions (Didan 2015), which is especially important as the study area is predominantly covered by dense miombo woodland (Goyder et al. 2018). The MODIS NDVI and EVI products are computed from atmospherically corrected bidirectional surface reflectance that have been masked for water, clouds, heavy aerosols, and cloud shadows (Didan 2015). The products contain a detailed quality assurance bitmask, which measures the reliability of the data. Data which is considered "good" or "useful" were kept (Didan 2015), whereas data which was contaminated by clouds were removed from the analysis. The MODIS NDVI and EVI data were used to generate time series, where values were removed due to cloud contamination, missing values

Table 1 SPI scores and classification (Svoboda et al., 2012)

SPI value	Classification
> 2.0	Extremely wet
1.5 to 1.99	Very wet
1.0 to 1.49	Moderately wet
− 0.99 to 0.99	Near normal
− 1.0 to − 1.49	Moderately dry
− 1.5 to − 1.99	Severely dry
≤ 2.0	Extremely dry

were replaced by the average of the values on either side of the contaminated period.

NDVI and EVI maps over the study area were produced using ArcMap 10.2. Due to the heterogeneity of vegetation coverage in the study area, vegetation indices cover three separate vegetation regions. These are (1) the highlands vegetation region which represents the entire study area; (2) the miombo vegetation; and (3) the valley vegetation. The total monthly precipitation and the monthly vegetation indices were tested for normality; all data was deemed to be not normally distributed according to the Shapiro Wilk Test ($p < 0.05$). Spearman Rank correlations between precipitation and the different vegetation regions were calculated to determine which vegetation region is more responsive to the seasonal precipitation of the area.

3 Results

3.1 Precipitation in the Angolan Highlands

The mean annual precipitation over the study area is 1113 mm for the period 1981–01-01 to 2020–12-31. The highest annual precipitation (1295 mm) is recorded in the Northwest and Northeast regions of the study area (Fig. 2). The landscape has distinct topographical features dominated by river processes; high elevations exist adjacent to low lying river valleys. Precipitation in the region is closely related to latitude and altitude. Both precipitation and altitude decrease towards the Southeast where the annual precipitation is lowest (904 mm). The CHIRPS data confirm the strong seasonality in precipitation for the Angolan highlands. For this study, we define the beginning of the wet season as the first month of precipitation occurrence following an extended dry period during a calendar year. According to the CHIRPS data, precipitation starts during September each year, reaching a peak in January (mean cumulative precipitation 231 mm/month). The wet season lasts through to April, and an almost entirely dry season lasts from May to August (Fig. 2c). The seasonality of precipitation for the Angolan highlands is applied to subsequent results.

3.2 Assessment of drought frequency

3.2.1 Drought events according to the SPI

To demonstrate the occurrence of drought at different timescales, the SPIs were calculated at 3-, 6-, 12-, and

Fig. 2 **a** The mean annual precipitation (mm/year) over the study site, **b** digital elevation model at 30 m resolution, and **c** the mean cumulative precipitation (mm/month) over the period 1981–01-01 to 2020–12-31. See supplementary material Fig. 1 for the full daily precipitation time series
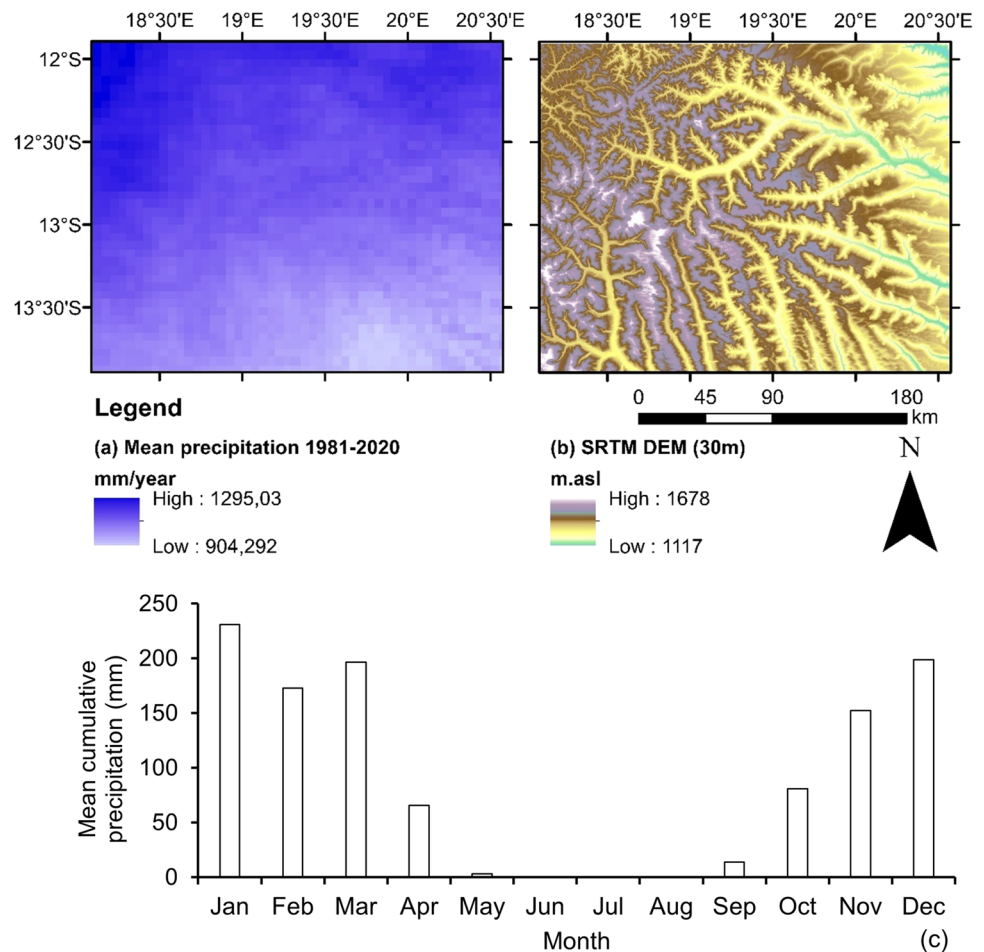
24-month timescales (Fig. 3). There are multiple drought events across the four timescales. For the 3-month SPI, a total of 37 drought events were recorded, 20 lasted at least three months of which three events occurred during the dry months from May to August. Three drought events lasted eight months during 1989–1990, 2014–2015, and 2018–2019, the longest drought event lasted 9 months from January 2017 to the end of September 2017. For the 6-month SPI, a total of 23 drought events were recorded, of which eight lasted at least 6 months. Two drought events were recorded for almost a full year (11 months) during 2014–2015 and 2018–2019, the longest drought event lasted 20 months from December 1995 to the end of July 1997.

For the 12-month SPI, a total of ten drought events were recorded, six lasted at least 12 months. Two 12-month drought events were recorded for 2008 and 2017–2018 and two 13-month events were recorded during 2015–2016 and 2019–2020. A 21-month long drought was recorded from February 2000 to the end of October 2001 and the longest

drought lasted for 45 months from April 1994 to the end of December 1997. For the 24-month SPI, three separate drought events were recorded over the precipitation archive. The shortest lasted for 21 months starting in January 2001 and ending in September 2002 and a 45-month drought lasted from April 1995 to the end of December 1998. The longest drought event lasting 70 months started in March 2015 and ended in December 2020, at the end of the precipitation record. See supplementary material Table 1 for details regarding drought start and end months, peak SPI, and drought magnitude over each SPI timescale.

3.2.2 Drought severity

For the 40-year period under observation (1981–2020) totalling 480 months, the number of months classified as either moderately, severely, or extremely dry were calculated (Table 2). Each of the SPI calculations had a similar total number of months (ranging between 76 and 83) classified as either moderately, severely, or extremely dry. The

Fig. 3 a–d The 3-, 6-, 12-, and 24-month SPI for the period 1981–01-01 to 2020–12-31. See supplementary material Fig. 2a-b for the 36-, 48-, 60-, and 96-month SPI plots
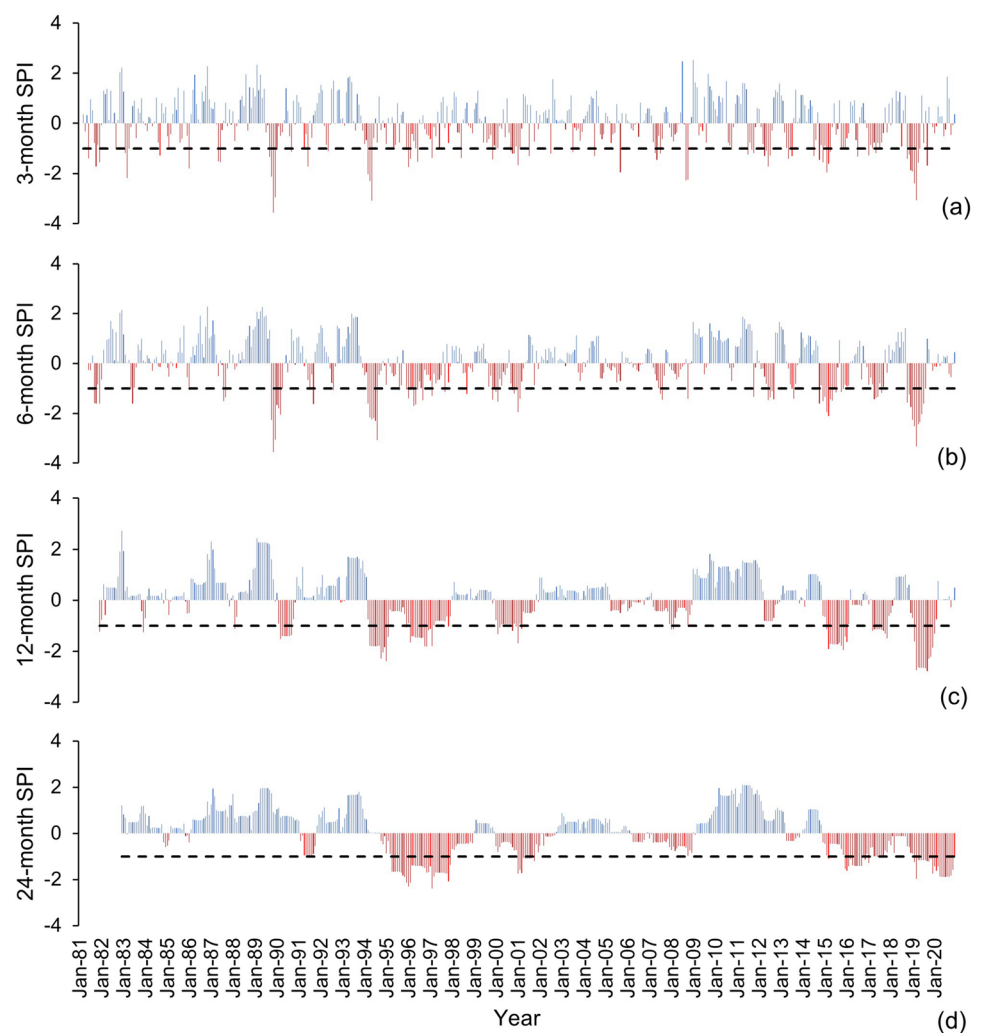
years that had the most months of drought conditions for the 3-month SPI occurred during 1989, 2000, 2012, 2015, 2017, and 2019; the 6-month SPI during 1994, 1996, 2000, 2012, 2015, 2017, and 2019; the 12 month during 1990, 1994, 1996, 2015, 2017, and 2019; and for the 24 month during 1995–1997, 2001, 2016, 2017, and 2019 and 2020.

3.2.3 Droughts and ENSO

There are eight common periods which met the threshold SPI scores for drought (Table 3), of which five reflected droughts which overlapped over all four (3-, 6-, 12-, and 24-month) separate SPI timescales. These eight common drought periods reflect drought events that lasted at least four months and occurred at the same time for at least two of the four SPI timescales. These eight common periods occurred during 1981–1982, 1989–1990, 1994, 1995–1997, 1999–2001, 2014–2016, 2017–2018, and 2018–2019. Five of these common drought periods are longer than 12 months, making it challenging to compare them to ENSO years. Only two drought periods (1994 and 2014–2016) coincided with specific El Niño years. The longest drought (1995–1997) coincided with a range of ENSO events including a moderate La Niña (1995–1996), an ENSO-neutral (1996–1997) and a very strong El Niño (1997–1998). An extended period of dryness lasted from October 2014 to February 2020 and included three separate common drought periods (2014–2016, 2017–2018, and 2018–2020).

3.3 Vegetation dynamics of the Angolan Highlands

3.3.1 Vegetation distribution and seasonality

Vegetation in the Angolan Highlands varies spatially along the distinct topographical features on the landscape (Fig. 4). The vegetation that grows in the river valleys has lower mean EVI (0.28) and NDVI (0.37) values than the surrounding miombo vegetation (0.53 and 0.72 respectively). The indices span three vegetation regions: (1) the miombo vegetation; (2) the valley vegetation; and (3) the combination of these termed highlands vegetation. The miombo vegetation grows adjacent to the river valley environments and is commonly depicted in green in Fig. 4, valley vegetation is shown by either yellow or red in Fig. 4 owing to the differences in vegetation index scores.

The seasonality of precipitation, EVI and NDVI are similar, with NDVI and EVI for all vegetation regions being lowest at the end of the dry winter months (August), and highest during the summer rainy season (Fig. 5). Vegetation scores are shown to increase at the start of the wet season in September. Peak precipitation and peak EVI scores are both calculated for January, peak NDVI for the miombo vegetation is shown to occur during April, nearer the end of the wet season.

A Spearman rank correlation matrix was produced for the total monthly precipitation and the monthly vegetation indices over the archive (Table 4). A stronger correlation exists between EVI highlands and precipitation (0.90) versus NDVI highlands and precipitation (0.75). The strongest correlation coefficient for precipitation is with EVI valley (0.92), EVI highlands (0.90) and NDVI valley (0.88). NDVI miombo has the weakest correlation coefficients with precipitation (0.57) and the other variables. With regards to the vegetation regions, the valley region has the strongest correlation between EVI and NDVI (0.96), followed by the highlands region (0.78) and then the miombo, having the weakest correlation (0.57).

3.3.2 Vegetation response to drought

The seasonality of vegetation and precipitation is similar; however, high, or low precipitation in each rainfall season does not imply high or low mean NDVI and EVI scores respectively. Starting in September 2000 and ending in August 2020, the rainfall for each rainfall season is variable (mean of 1110 ± 91 mm/year). The driest rainfall seasons occurred during 2018/2019 (888 mm), 2014/2015 (962 mm), and 2016/2017 (1010 mm). By comparison, lowest mean NDVI scores for the highlands vegetation region occurred during 2000/2001 (0.6358), 2008/2009 (0.6365), and 2003/2004 (0.6367) and lowest EVI mean scores for the highlands vegetation region occurred during 2009/2010 (0.3275), 2003/2004 (0.3323), and 2011/2012 (0.3371).

The vegetation time series reflects that interannual vegetation dynamics are consistent with precipitation in the Angolan Highlands (Fig. 6). Low mean NDVI and EVI scores occurred at the beginning of the time series during the drought event lasting from November 1999 to October 2001 over all vegetation regions. These low vegetation scores reflected during the end of the dry seasons in August 2000 and 2001, although the decrease in vegetation scores during the dry season are not specific to drought events. The extended dry period from October 2014 to February 2020 would have potentially placed vegetation in the highlands under strain. Vegetation index scores indicate that during this period, the vegetation over all regions was able to recover at the start of each rainfall season. Vegetation recovery in the highlands was especially evident during the 2018/2019 rainfall season (888 mm, the lowest on record over the full 40-year archive) where both EVI and NDVI scores were comparatively low during the dry season but recovered at the start of the 2019/2020 season.

Table 2 Number of months classified as either moderately, severely, or extremely dry per year according to the respective SPI calculations

Year	3-month SPI				6-month SPI				12-month SPI				24-month SPI			
SPI Classification	Moderate	Severe	Extreme	Total	Moderate	Severe	Extreme	Total	Moderate	Severe	Extreme	Total	Moderate	Severe	Extreme	Total
1981	1	2	–	3	–	3	–	3	1	–	–	1	–	–	–	–
1982	–	–	–	–	–	–	–	–	–	–	–	–	–	–	–	–
1983	2	–	1	3	–	1	–	1	1	–	–	1	–	–	–	–
1984	1	–	–	1	–	–	–	–	–	–	–	–	–	–	–	–
1985	–	–	–	–	–	–	–	–	–	–	–	–	–	–	–	–
1986	–	1	–	1	1	–	–	1	–	–	–	–	–	–	–	–
1987	–	2	–	2	1	1	–	2	–	–	–	–	–	–	–	–
1988	–	–	–	–	–	–	–	–	1	–	–	1	–	–	–	–
1989	1	–	3	4	–	–	3	3	–	–	–	–	–	–	–	–
1990	2	–	–	2	–	2	1	3	6	1	–	7	–	–	–	–
1991	–	1	–	1	–	1	–	1	–	–	–	–	–	–	–	–
1992	1	–	–	1	1	–	–	1	–	–	–	–	–	–	–	–
1993	–	–	–	–	–	–	–	–	–	–	–	–	–	–	–	–
1994	–	–	3	3	–	1	5	6	–	7	2	9	–	–	–	–
1995	2	–	–	2	2	–	–	2	2	–	1	3	–	8	1	9
1996	1	2	–	3	4	2	–	6	8	3	–	11	8	2	2	12
1997	2	–	–	2	2	–	–	2	2	1	–	3	2	8	2	12
1998	1	–	–	1	1	–	–	1	–	–	–	–	–	–	–	–
1999	1	–	–	1	1	–	–	1	–	–	–	–	–	–	–	–
2000	4	–	–	4	4	1	–	5	4	–	–	4	–	–	–	–
2001	1	1	–	2	1	1	–	2	1	1	–	2	7	3	–	10
2002	1	–	–	1	–	–	–	–	–	–	–	–	–	–	–	–
2003	1	–	–	1	–	–	–	–	–	–	–	–	–	–	–	–
2004	1	–	–	1	–	–	–	–	–	–	–	–	–	–	–	–
2005	–	–	–	–	–	–	–	–	–	–	–	–	–	–	–	–
2006	–	–	–	–	–	–	–	–	–	–	–	–	–	–	–	–
2007	3	–	–	3	2	–	–	2	–	–	–	–	–	–	–	–
2008	–	–	2	2	1	–	–	1	3	–	–	3	–	–	–	–
2009	–	–	–	–	–	–	–	–	–	–	–	–	–	–	–	–
2010	1	–	–	1	1	–	–	1	–	–	–	–	–	–	–	–
2011	3	–	–	3	1	–	–	1	–	–	–	–	–	–	–	–
2012	3	1	–	4	4	–	–	4	–	–	–	–	–	–	–	–
2013	3	–	–	3	2	–	–	2	2	–	–	2	–	–	–	–
2014	2	1	–	3	–	2	–	2	–	–	–	–	–	–	–	–
2015	3	2	–	5	7	1	1	9	2	9	–	11	1	1	–	2

Table 2 (continued)

Year	SPI Classification	3-month SPI				6-month SPI				12-month SPI				24-month SPI			
		Moderate	Severe	Extreme	Total	Moderate	Severe	Extreme	Total	Moderate	Severe	Extreme	Total	Moderate	Severe	Extreme	Total
2016		1	–	–	1	–	–	–	1	–	1	–	1	10	1	–	11
2017		4	–	–	4	4	–	–	4	8	1	–	9	5	–	–	5
2018		2	1	–	3	2	1	–	3	–	–	–	–	–	–	–	–
2019		1	3	2	6	6	1	1	8	–	2	9	11	9	2	–	11
2020		–	–	–	–	–	–	–	–	1	–	–	1	2	9	–	11
Total		49	18	11	78	47	18	11	76	42	26	12	80	44	34	5	83

4 Discussion

4.1 Drought events and synoptic drivers of drought

This is the first study to analyze drought occurrence in the Angolan Highlands. The 3-, 6-, 12-, and 24-month SPIs reached drought conditions on multiple occasions over the 40 years, revealing eight common drought periods: 1981–1982, 1989–1990, 1994, 1995–1997, 1999–2000, 2014–2016, 2017–2018, and 2018–2020. The benefit of this hindsight lies in exposing the cause of these droughts to improve forecasting capability. There are large-scale synoptic systems that influence precipitation in the region. The seasonal precipitation starts during the austral winter when a heat low develops over the Bie Plateau causing advection of moist tropical westerlies from the Atlantic Ocean and the Congo Basin (Rouault et al. 2003; Cook et al. 2004; Howard and Washington 2018). Moist air from the tropical Indian Ocean is brought by the easterly trade winds resulting in a convergence known as the Congo Air Boundary (Howard and Washington 2018; Crétat et al. 2019). As summer approaches, the Congo Air Boundary migrates southward, and the heat low dissipates to be replaced by the semi-transient Angola Low (Howard and Washington 2018).

Weakening of the Congo Air Boundary during summer allows the heat low to effectively migrate southward over Namibia, removing the moisture barrier from the tropics (Howard and Washington 2018; Crétat et al. 2019). The moisture sources from the westerlies and the Congo Basin diminishes relative to the increased moisture supply from the Indian Ocean and easterlies, meaning that the Angola Low becomes the focal point of the southward development of convective systems. These mature as temperate tropical troughs (TTTs) that provide rainfall over much of the African subcontinent in the summer months (Harrison, 1984; Todd and Washington 1999; James et al. 2020). In this way, the Angola Low has a strong influence on regional precipitation across Southern Africa (Mulenga 1999). The Angola Low is centered around 13°S, 20°E (Howard and Washington 2018) directly above the Angolan Highlands study area.

Howard and Washington (2018) characterize the Angola Low as a combination of early-season heat low events (Angola heat low) and late-season tropical low events (Angola tropical low). The dry-convection Angola heat low occurs from October to November and transitions to the moist-convection Angola tropical low during December, remaining until March. The heat lows appear to be geographically locked and form only over Angola, whereas the tropical lows travel east to west across the African continent but linger at around 20°E (Howard and Washington 2018). The Angola tropical low is important for southern Africa rainfall and are dynamically similar to monsoon low

Table 3 Common drought periods according to each SPI calculation and ENSO years

Year	Drought start and end month	Duration (months)	Year-long/wet /dry season drought	Max. SPI classification, SPI overlap (max. =4)	ENSO (year), *SST anomaly strength (NOAA, 2021, 2022)
1981–82	Oct '81–Jan '82	4	Wet	Severe, 3	Neutral (1980–1982)
1989–90	Oct '89–May '90	8	Wet	Extreme, 3	Neutral (1989–1990)
1994	Mar '94–Oct '94	8	Wet + Dry	Extreme, 3	El Niño (1994–1995), moderate
1995–97	Apr '95–Sep '97	33	Multiple year	Extreme, 4	La Niña (1995–1996), moderate. Neutral (1996–1997). El Niño (1997–1998), very strong
1999–01	Nov '99–Oct '01	24	Multiple year	Extreme, 4	La Niña (1999–2000), strong. La Niña (2000–2001), weak
2014–16	Oct '14–Feb '16	17	Year-long	Extreme, 4	El Niño (2014–2015), weak. El Niño (2015–2016), very strong
2017–18	Jan '17–Feb '18	14	Year-long	Extreme, 4	La Niña (2017–2018), weak
2018–20	Oct'18–Feb'20	17	Year-long	Extreme, 4	El Niño (2018–2019), weak. Neutral (2019–2020)

*ENSO SST anomaly strength classification: weak (0.5 to 0.9 SST anomaly), moderate (1.0 to 1.4), strong (1.5 to 1.9), and very strong ($\geq$ 2.0: NOAA, 2021)

Fig. 4 Mean **a** EVI and **b** NDVI over the study area for the period 2000–02-18 to 2020–12-31
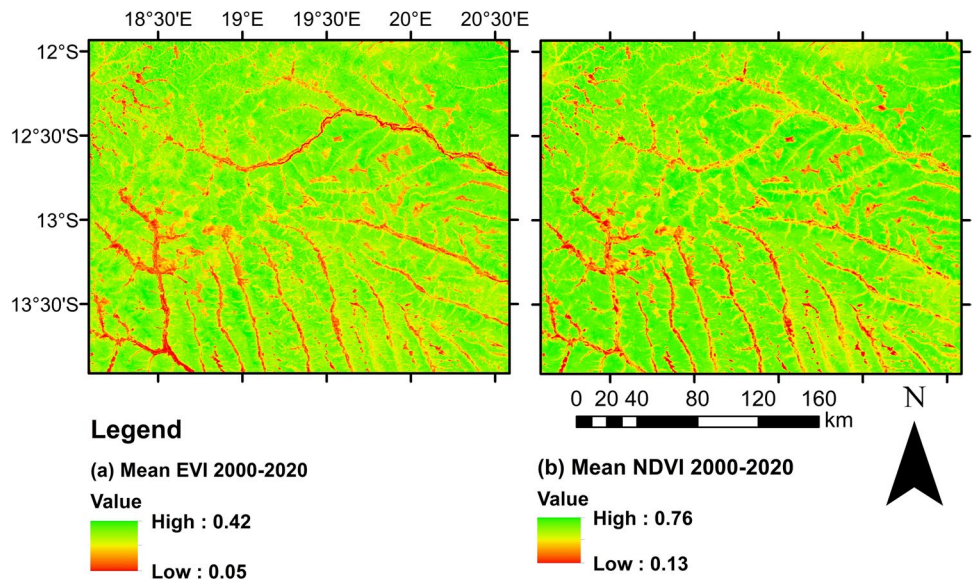
Fig. 5 The CHIRPS mean daily precipitation for each month across the Angolan Highlands study area from 1981–01-01 to 2020–12-31 and the mean NDVI and EVI for each month for the period 2000–02-18 to 2020–12-31 across the three vegetation regions
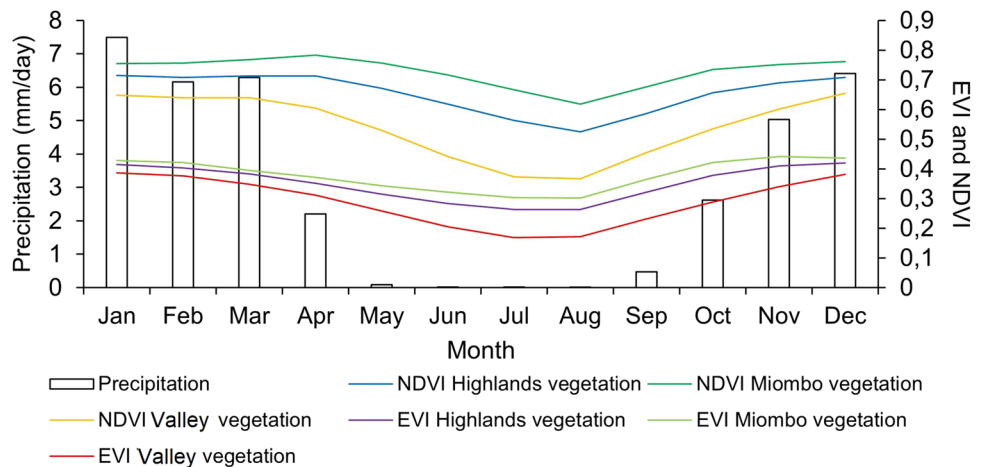
Table 4 Correlation matrix between vegetation indices and precipitation

Variables	EVI Highlands	EVI Miombo	EVI Valley	NDVI Highlands	NDVI Miombo	NDVI Valley	Precipitation
EVI Highlands	1						
EVI Miombo	0.965	1					
EVI Valley	0.947	0.874	1				
NDVI Highlands	0.780	0.683	0.861	1			
NDVI Miombo	0.642	0.571	0.708	0.925	1		
NDVI Valley	0.883	0.794	0.962	0.932	0.802	1	
Precipitation	0.896	0.842	0.918	0.750	0.565	0.875	1

All values presented are different from 0 with a significance level alpha = 0.05 ($p < 0.005$)

Fig. 6 **a** The mean NDVI and **b** EVI for each vegetation region per month, the total precipitation per month, and the common drought periods over the period (2000–02-18 to 2020–12-31)
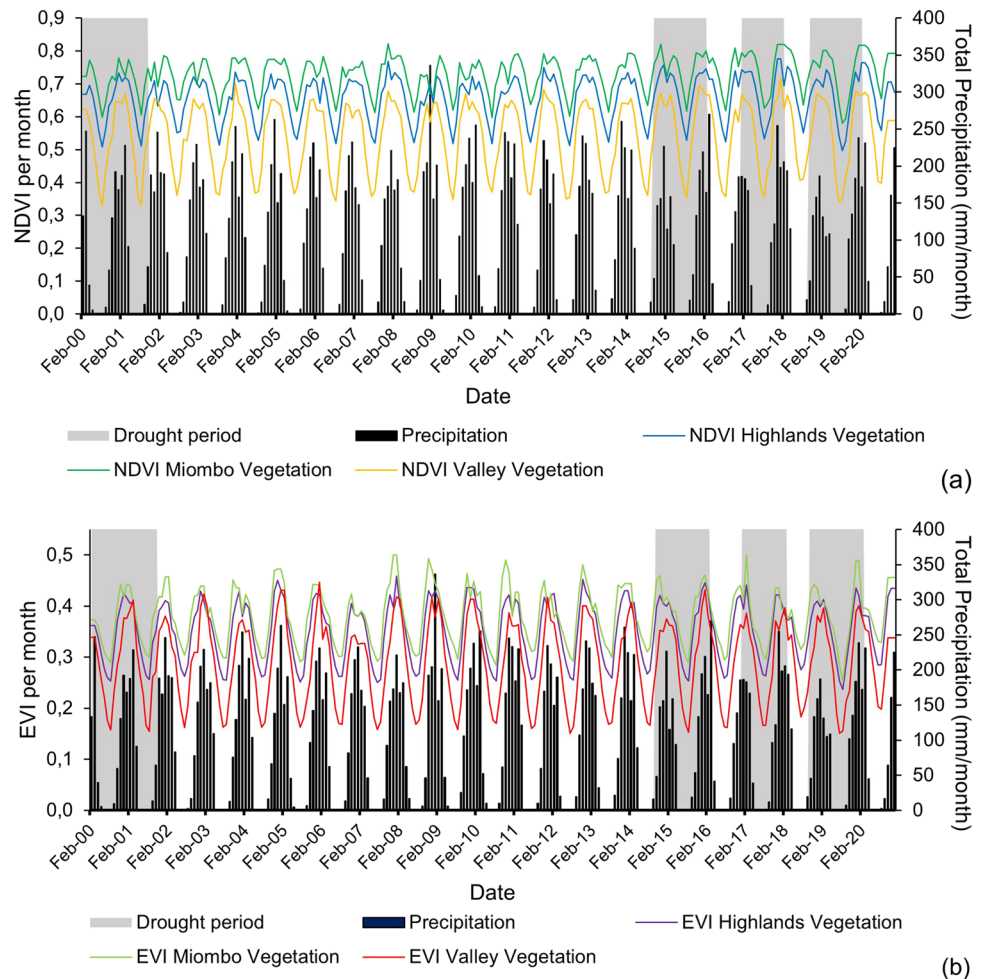
pressure systems found in tropical landmasses (Howard and Washington 2018).

The El Niño phase of ENSO is typically associated with drought in southern Africa, a result of the shift in the Walker circulation (Rouault and Richard 2005). Reason and Jagadheesha (2005) found that the Angola Low may have a modulating impact on the relationship between southern Africa precipitation and ENSO. The dynamics of the Angola Low vary in intensity and location, the

1982–1983 and 2015–2016 El Niño events both occurred in years where the Angola Low was weak and resulted in severe drought over Angola (Howard and Washington 2018). The SPI results indicate that drought events over the Angolan highlands occurred before 1982–1983, in 1981–1982, and during 2014–2016. By contrast, the 1997–1998 El Niño coincided with a strong Angola Low and a drought was not observed (Howard and Washington 2018). The SPI indicates that a period of non-drought

conditions occurred between October 1997 and October 1999 over the study area. Lyon and Mason (2007) confirmed the role of the Angola Low with regards to ENSO and precipitation and found that high sea surface temperatures near southern Africa and anomalous shifts in Walker circulation contributed to the increase in precipitation in 1997–1998 as compared to 1982–1983.

The first two common drought events over the Angolan Highlands (1981–1982 and 1989–1990) occurred during ENSO neutral years. The 1994 drought coincides with a moderate El Niño event during 1994–1995 (Blamey et al. 2018; NOAA 2021), and is consistent with drought conditions over the southern African region (Rouault and Richard 2005; Tirivarombo et al. 2018). The 1995–1997 drought coincided with La Niña years, ENSO neutral years, and the 1997–1998 El Niño, which was the strongest in the twentieth century (Thomson et al. 2003; Blamey et al. 2018; NOAA 2021). The 1995–1997 drought lasting 33 months had 31 months classified as extremely dry (SPI value ≤ 2.0) for at least one SPI timescale. In southern Africa, the El Niño event of 1997–1998 was associated with an above average summer rainfall season (Blamey et al. 2018) and numerous semi-transient tropical lows over the summer months (Howard and Washington 2018). The 1997–1998 rainfall season also had above average precipitation (1130 mm vs. 1114 mm) compared to the 40-year archive for the Angolan Highlands.

Over Southern Africa, an extremely wet La Niña summer of 1999–2000 featured several tropical low events, particularly Tropical Cyclone Eline which caused devastating floods in Mozambique, Zimbabwe, and South Africa (Reason and Keibel 2004). The tropical cyclone tracked across Southern Africa from Mozambique and dissipated in eastern Namibia (Reason and Keibel 2004), evidently not influencing the Angolan Highlands as the SPI reached drought conditions lasting from November 1999 to October 2001. The 1999–2001 drought period in the Angolan Highlands is consistent with severe drought reported for Angola (Rouault and Richard 2005). However, this drought period does not coincide with other southern African countries such as Zimbabwe, Lesotho, South Africa, Zambia, and Botswana, which experienced severe drought later in 2002, 2003, and 2004, during which low crop production led to a serious threat on food security (Rouault and Richard 2005). By comparison, the SPI suggests that drought conditions did not persist into 2002 in the Angolan Highlands. The period between 2002 and 2004 was shown to have positive SPI scores, indicative of wet conditions.

The results of this study indicate that drought events have become more frequent in the Angolan Highlands over the past decade. The region suffered severe drought during 2014–2016, consistent with drought conditions in the wider southern African region (Mlenga et al. 2019), and coincident with one of the strongest El Niño events on record during 2015–2016 (Blamey et al. 2018; Kolusu et al. 2019; NOAA 2021). The regional event was the driest in the historical record (Blamey et al. 2018), which was compounded by dry conditions over the previous year (Kolusu et al. 2019). El Niño events typically lead to drier conditions during January, February, and March at the end of the summer season (Blamey et al. 2018). The SPI for the Highlands indicate that dry conditions began at the start of the rainy season in October 2014, consistent with what was identified throughout the southern African region during the 2015–2016 El Niño event (Blamey et al. 2018; Kolusu et al. 2019). The contrasting rainfall patterns and inconsistent connection between El Niño events and southern African climate is well documented (Boulard et al. 2013; Blamey et al. 2018), and the evidence from the Angolan Highlands is similarly erratic.

Droughts do not necessarily fall into single seasons and droughts typically end during the wet season (Luetkemeier and Liehr 2019). The dry months of 2017 (May through August) during the drought from January 2017 to February 2018 were classified as moderately dry, while positive scores for March 2018 signal that the drought terminated late in the rainfall season. Dry conditions were exacerbated by low precipitation over the next rainfall season, and another extreme drought started in October 2018. During 2019, it was documented that the southern provinces of Angola had one of the driest seasons since at least 1981 (RVAA, 2019). This is consistent with the average precipitation per rainfall year across the Angolan Highlands, where the 2018–2019 rainfall season (888 mm) was the lowest on record over the full 40-year archive. This recent drought event has had serious implications on food security and health in the southern provinces of Cunene, Hulia, and Namibe (RVAA 2019), and the SPI demonstrates that this was a widespread phenomenon extending to the Angolan Highlands.

4.2 Drought implications

NDVI and EVI historical data were used to assess the impacts of precipitation deficits on vegetation over the Angolan Highlands. EVI minimizes canopy background variations and maintains sensitivity over dense vegetation conditions (Didan 2015), whereas NDVI tends to overestimate vegetation growth over densely vegetated areas and is also sensitive to underlying soil colour (Gao et al. 2020). EVI is more strongly correlated to precipitation than NDVI in the region, potentially caused by overestimation of miombo vegetation over certain months by the NDVI. The heterogenous vegetation cover led to the analysis of three different vegetation regions: the highlands, miombo, and valley vegetation. The miombo woodlands contain over 8500 plant species, provide habitat for wildlife, and support millions of people who are dependent on the woodlands for their livelihoods

(WWF 2021). NDVI for miombo vegetation has the weakest correlation with precipitation, and the seasonality suggests that miombo vegetation reaches greatest productivity in April, 3 months after the wettest month suggesting a lag time in miombo productivity.

Valley vegetation for both NDVI and EVI has the strongest correlation to precipitation. The valley environment supports extensive riparian vegetation including wet grasslands, peatlands, and oxbow lakes (Conradie et al. 2016; Goyder et al. 2018). Lourenco et al (2022) describe the peatlands as minerotrophic, a distinct seep-line exists parallel to the higher ground (dominated by miombo vegetation) adjacent to the valley region, the seep-line is an inflow area of ground water, and peatlands persist where there are physical features that pond this water. The valley environment is often patchy, having less peatland cover in comparison to much larger expanses of grassland (Lourenco et al. 2022). The seasonal response of valley vegetation suggests that areas that are not ponded are dependent on precipitation, having a similar seasonal pattern to precipitation.

The strong correlation between vegetation indices and precipitation demonstrates the potential risks to regional vegetation during periods of drought. During 2019, the Angola Vulnerability Assessment Committee mention that the drought caused loss of livestock and low crop yields in the southern provinces of Angola (RVAA 2019). It was estimated that 1.14 million people were food insecure in the southern provinces of Namibe, Cunene, Cuando Cubango, and Huila alone, and it is likely that the subsistence communities in the Angolan Highlands experienced the same hardships. Total precipitation and drought frequency are important factors in determining total greenness for a given time, but they do not operate in isolation. Despite the results indicating that drought events have become more frequent in the Angolan Highlands over the last decade, it is possible that vegetation growth may be enhanced by CO_2 fertilization and improved water efficiency as documented in tropical, woodland and savanna biomes across southern Africa (Midgley and Thuiller 2011; Jin et al. 2013; Geremew et al. 2022).

The threat of drought to the Angolan Highland landscape is further exacerbated by anthropogenic practices. The miombo vegetation is cleared for timber and the valley environment is used for cultivation through peatland drainage, peat fuel is also extracted, and grassland areas are used for grazing and often burned (Conradie et al. 2016; Taylor et al. 2018). Significant societal impacts are common amongst food-scarce developing countries with high dependency on agriculture (Ahmadalipour et al. 2019). Increased drought occurrence could have major impacts in a region that is heavily dependent on natural resources. Continued population growth, lack of financial support, subsistence agriculture, and human pressure on the land are increasing in unprotected, rural areas of Angola (Catarino et al.

2020), such as the Angolan Highlands. The rural population of Angola comprises 11.1 million people, or 37% of the total population (RVAA 2019). According to the International Trade Administration (ITA), in 2018, agriculture accounted for 11% of the country's GDP, supporting both informal and formal employment of 30% of the Angolan population (ITA 2021). Potential environmental degradation can be expected from the combination of drought and anthropogenic pressures. This will require adaptation strategies in future, especially concerning water resources and agricultural practices.

4.3 Threats of climate change

Angola is highly vulnerable to climate change (Brooks et al. 2005). Climate variability in the Angolan Highlands region is one of the strongest drivers of rainfall variability over a subcontinent (Crétat et al. 2019). The trends in SPI scores indicate negative gradients towards drier conditions over all timescales. Over the archive, drought return rates are variable but have increased during the last decade, as three separate drought events occurred since 2014. This data is consistent with other studies for Angola, both stronger and more frequent droughts are expected through the next century (Brooks et al. 2005; Cain 2015; Carvalho et al. 2017). Due to the paucity of monitoring networks, studies of climate projections in Africa rarely include Angola, the majority of which provide an evaluation of different regional climate models (RCMs) over multiple countries (Carvalho et al. 2017).

Carvalho et al. (2017) compared four RCMs with data from 12 meteorological monitoring stations specifically in Angola. The study presented scenarios of future temperature and precipitation anomaly trends and the frequency and intensity of droughts for the twenty-first century. While there is a difference in the performance of the four RCMs, particularly for precipitation, consistent results were found for temperature projections, with an increase of up to 4.9 °C by 2100 (Carvalho et al. 2017). The temperature increases are lowest for the northern coastal areas and highest for the southeast areas (nearer the study site). In addition to increased temperatures, Angola is predicted to face heat waves lasting between 60 and 120 days every 2 years under the RCP8.5 (business as usual) scenario (Dosio 2017). In contrast to temperature increases, precipitation is projected to decrease by 2% on average for the country. Once more, the strongest projection was for the southeast, with decreases of up to 4% (Carvalho et al. 2017).

Using the 6- and 12-month SPI data and RCMs, Carvalho et al. (2017) concluded that climate change in Angola will bring stronger and more frequent droughts (consistent with the SPI data for the Angolan highlands) through the century, with impacts on water resources, agricultural productivity, and wildfire potential. Mendelsohn (2019) describes the current challenges to land transformation and degradation in

Angola that are likely to increase in future (Carvalho et al. 2017; Huntley et al. 2019). The need for fuel sources reduces plant cover, resulting in lower volumes of rainwater being trapped or impeded, thus reducing seepage into the topsoil to replenish soil moisture and recharge local aquifers (Mendelsohn, 2019; Huntley et al. 2019). With lower soil moisture, seepage to sustain river flows during the dry season also declines (Huntley et al. 2019). As precipitation affects productivity, this will have influence on the subsistence farming strategy, and crop production. This may be the reason for increased farming of peatlands which are an important carbon sink and water flow regulator (Lourenco et al. 2022), leading to further environmental degradation.

The lack of reliable climate data for Angola from the past 40 years is a challenge for climate change research (Huntley et al. 2019). The Angolan Highlands are hydrologically and ecologically important but continue to remain unprotected (Quammen 2017). It is a major source water region for three major river catchments (Congo, Zambezi, and Okavango), supporting transboundary rivers that flow into six southern African countries (Namibia, Botswana, Zambia, the Democratic Republic of the Congo, Mozambique, and Zimbabwe) and is the only source region of the Okavango Delta (Marazzi et al. 2017; Yurco et al. 2017). Drought events occurring in the region are likely to be far reaching, affecting human and ecological welfare downstream. The rivers originating in the highlands continue to flow unimpeded but future pressures on water resources and projected population increases are likely to aggravate dwindling freshwater reserves in southern Africa. Synoptic drivers of precipitation in the region have only recently received strong attention (Howard and Washington 2018; Crétat et al. 2019). Future work in monitoring and protecting the highlands will have strong implications for water budgets across southern Africa.

5 Conclusion

This study integrates precipitation data and vegetation indices in an historical assessment of drought in the Angolan Highlands. Drought occurrence has increased over the last four decades, with three drought events occurring since 2014. The SPI data indicates that most of the drought periods were regional. The relationship between drought occurrence and ENSO is not linear. A strong positive correlation exists between vegetation and precipitation, with EVI having the stronger correlation over NDVI and precipitation. The valley vegetation has a stronger correlation with precipitation compared to the miombo vegetation, reflecting the same seasonality as precipitation. The observed SPI time series exhibited a downward trend during the past 40 years. Although 40 years is a relatively short period with regard to decadal and multi-decadal climate variability, this could support the

notion that drought occurrence and frequency will increase in future as determined in other studies. Drought incidence and severity should be carefully monitored, representing a key future avenue for climate modelling research in the region. Despite the significant ecological importance of the Angolan highlands, the region remains unprotected. The Angolan population is reliant on rain-fed agriculture, adaptive measures, especially for water resources are required to mitigate the impacts of future drought events.

Declarations

References

Abiodun BJ, Makhanya N, Petja B, Abatan AA, Oguntunde PG (2019) Future projection of droughts over major river basins in Southern Africa at specific global warming levels. Theoret Appl Climatol 137(3):1785–1799. https://doi.org/10.1007/s00704-018-2693-0

AghaKouchak A, Mirchi A, Madan K, Di Baldassarre G, Nazemi A, Alborzi A et al. (2021). Anthropogenic drought: definition, challenges and opportunities. Reviews of Geophysics, 59(2) https://doi.org/10.1029/2019RG000683

Ahmadalipour A, Moradkhani H, Castelletti A, Magliocca N (2019) Future drought risk in Africa: integrating vulnerability, climate change, and population growth. Sci Total Environ 662:672–686. https://doi.org/10.1016/j.scitotenv.2019.01.278

Alamdarloo EH, Manesh MB, Khosravi H (2018) Probability assessment of vegetation vulnerability to drought based on remote sensing data. Environ Monit Assess 190(12):1–11. https://doi.org/10.1007/s10661-018-7089-1

Bachmair S, Stahl K, Collins K, Hannaford J, Acreman M, Svoboda M et al (2016) Drought indicators revisited: the need for a wider consideration of environment and society. Wiley Interdiscip Rev: Water 3(4):516–536

Blamey RC, Kolusu SR, Mahlalela P, Todd MC, Reason CJC (2018) The role of regional circulation features in regulating El Niño climate impacts over southern Africa: a comparison of the 2015/2016 drought with previous events. Int J Climatol 38:4276–4295. https://doi.org/10.1002/joc.5668

Boulard D, Pohl B, Crétat J, Vigaud N, Pham-Xuan T (2013) Downscaling large-scale climate variability using a regional climate model: the case of ENSO over southern Africa. Clim Dyn 40:1141–1168. https://doi.org/10.1007/s00382-012-1400-6

Brooks N, Adger WN, Kelly PM (2005) The determinants of vulnerability and adaptive capacity at the national level and the implications for adaptation. Glob Environ Chang 15:151–163. https://doi.org/10.1016/j.gloenvcha.2004.12.006

Brown JF, Wardlow BD, Tadesse T, Hayes MJ, Reed BC (2008) The vegetation drought response index (VegDRI): a new integrated approach for monitoring drought stress in vegetation. Gisci Remote Sens 45(1):16–46. https://doi.org/10.2747/1548-1603.45.1.16

Cain A (2015) Climate Change & Land Markets in Coastal Cities of Angola–the case of Luanda. In World Bank conference on land and poverty, The World Bank, Washington, DC

Carvalho SCP, Santos FD, Pulquério M (2017) Climate change scenarios for Angola: an analysis of precipitation and temperature projections using four RCMs. Int J Climatol 37(8):3398–3412. https://doi.org/10.1002/joc.4925

Catarino S, Romeiras MM, Figueira R, Aubard V, Silva J, Pereira J (2020) Spatial and temporal trends of burnt area in Angola: implications for natural vegetation and protected area management. Diversity 12(8):307–329. https://doi.org/10.3390/d12080307

Conradie W, Bills R, Branch WR (2016) The herpetofauna of the Cubango, Cuito, and lower Cuando river catchments of southeastern Angola. Amphibian Reptile Conserv 10(2):6–36

Cook C, Reason CJC, Hewitson BC (2004) Wet and dry spells within particularly wet and dry summers in the South African summer rainfall region. Climate Res 26(1):17–31. https://doi.org/10.3354/cr026017

Crétat J, Pohl B, Dieppois B, Berthou S, Pergaud J (2019) The Angola low: relationship with southern African rainfall and ENSO. Clim Dyn 52(3–4):1783–1803. https://doi.org/10.1007/s00382-018-4222-3

Didan K (2015) MOD13Q1 MODIS/Terra vegetation indices 16-Day L3 Global 250m SIN Grid V006. Distributed by NASA EOSDIS Land Processes DAAChttps://doi.org/10.5067/MODIS/MOD13Q1.006

Didan K, Munoz AB, Solano R and Huete A (2015) MODIS vegetation index user's guide (MOD13 series). University of Arizona: Vegetation Index and Phenology Lab. Available at: https://lpdaac.usgs.gov/documents/103/MOD13_User_Guide_V6.pdf (Accessed 24 May 2022).

Dosio A (2017) Projection of temperature and heat waves for Africa with an ensemble of CORDEX regional climate models. Clim Dyn 49(1):493–519. https://doi.org/10.1007/s00382-016-3355-5

Ebi KL, Bowen K (2016) Extreme events as sources of health vulnerability: drought as an example. Weather Climate Extremes 11:95–102. https://doi.org/10.1016/j.wace.2015.10.001

Edwards DC and McKee TB (1997) *Characteristics of 20th century drought in the United States at multiple time scales*. Climatology Report 97–2, Department of Atmospheric Science, Colorado State University, Fort Collins, Colorado.

Food and Agriculture Organisation of the United Nations (FAO) (2021) The Republic of Angola. Drought expected to significantly reduce cereal production and pasture availability, with severe consequences for food security in 2021. https://reliefweb.int/sites/reliefweb.int/files/resources/cb4382en.pdf. Accessed 12 September 2021.

Funk C, Peterson P, Landsfeld M, Pedreros D, Verdin J, Shukla S et al (2015) The climate hazards infrared precipitation with stations—a new environmental record for monitoring extremes. Scientific Data 2:150066. https://doi.org/10.1038/sdata.2015.66

Gao L, Wang X, Johnson BA, Tian Q, Wang Y, Verrelst J, Xihan Mu, Xingfa Gu (2020) Remote sensing algorithms for estimation of fractional vegetation cover using pure vegetation index values: a review. ISPRS J Photogramm Remote Sens 159:364–377. https://doi.org/10.1016/j.isprsjprs.2019.11.018

Geremew T, Gonsamo A, Zewdie W, Pellikka P (2022) changing sensitivity of diverse tropical biomes to precipitation consistent with the expected carbon dioxide fertilization effect. J Landscape Ecol 15(1):78–93. https://doi.org/10.2478/jlecol-2022-0005

Gibbs WJ and Maher JV (1967) Rainfall deciles as drought indicators. Bureau of Meteorology Bulletin. 48. Commonwealth of Australia, Melbourne, Australia.

González J, Valdés J (2006) New drought frequency index: Definition and comparative performance analysis. Water Resour Res 42(11):W11421. https://doi.org/10.1029/2005WR004308

Gore M, Abiodun BJ, Kucharski F (2020) Understanding the influence of ENSO patterns on drought over southern Africa using SPEEDY. Clim Dyn 54:307–327. https://doi.org/10.1007/s00382-019-05002-w

Goyder DJ, Barker N, Bester SP, Frisby A, Janks M, Gonçalves F (2018) The Cuito catchment of the Okavango system: a vascular plant checklist for the Angolan headwaters. PhytoKeys 11:1–31. https://doi.org/10.3897/phytokeys.113.30439

Guttman NB (1999) Accepting the Standardized Precipitation Index: a calculation algorithm. J Am Water Resour Assoc 35(2):311–322. https://doi.org/10.1111/j.1752-1688.1999.tb03592.x

Harrison MSJ (1984) A generalized classification of South African summer rain-bearing synoptic systems. J Climatol 4(5):547–560. https://doi.org/10.1002/joc.3370040510

Howard E, Washington R (2018) Characterizing the synoptic expression of the Angola low. J Clim 31(17):7147–7165. https://doi.org/10.1175/JCLI-D-18-0017.1

Hua L, Wang H, Sui H, Wardlow B, Hayes MJ, Wang J (2019) Mapping the spatial-temporal dynamics of vegetation response lag to drought in a semi-arid region. Remote Sens 11(16):1873–1895. https://doi.org/10.3390/rs11161873

Huntley BJ, Russo V, Lages F, Ferrand N (2019) Biodiversity of Angola: Science & conservation: A modern synthesis. Springer Nature, p 549

International Trade Administration (ITA) (2021) Angola: agricultural products overview. https://www.privacyshield.gov/article?id=Angola-Agricultural-Products. Accessed 16 September 2021.

James R, Hart NC, Munday C, Reason CJC, Washington R (2020) Coupled climate model simulation of tropical–extratropical cloud bands over southern Africa. J Clim 33(19):8579–8602. https://doi.org/10.1175/JCLI-D-19-0731.1

Jin C, Xiao X, Merbold L, Arneth A, Veenendaal E, Kutsch WL (2013) Phenology and gross primary production of two dominant savanna woodland ecosystems in Southern Africa. Remote Sens Environ 135:189–201. https://doi.org/10.1016/j.rse.2013.03.033

Kchouk S, Melsen LA, Walker DW, van Oel PR (2022) A review of drought indices: predominance of drivers over impacts and the

importance of local context. Nat Hazards Earth Syst Sci Discuss 22:323–344. https://doi.org/10.5194/nhess-22-323-2022

Kolusu SR, Shamsudduha M, Todd MC, Taylor RG, Seddon D, Kashaigili JJ et al (2019) The El Niño event of 2015–2016: climate anomalies and their impact on groundwater resources in East and Southern Africa. Hydrol Earth Syst Sci 23(3):1751–1762. https://doi.org/10.5194/hess-23-1751-2019

Komuscu AU (1999) Using the SPI to analyze spatial and temporal patterns of drought in Turkey. Drought Network News, (1994–2001).49(1):7–11.

Liou YA, Mulualem GM (2019) Spatio–temporal assessment of drought in Ethiopia and the impact of recent intense droughts. Remote Sens 11(15):1828–1847. https://doi.org/10.3390/rs11151828

Lourenco M, Fitchett JM, Woodborne S (2022) Angolan highlands peatlands: extent, age and growth dynamics. Sci Total Environ 810:152315. https://doi.org/10.1016/j.scitotenv.2021.152315

Luetkemeier R, Liehr S (2019) Integrated responses to drought risk in Namibia and Angola. ISOE Policy Brief, No. 6. ISOE – Institute for Social-Ecological Research (ed). Frankfurt, Germany, pp 56–61

Lyon B, Mason SJ (2007) The 1997–98 summer rainfall season in southern Africa. Part i: Obs J Climate 20(20):5134–5148. https://doi.org/10.1175/JCLI4225.1

Marazzi L, Gaiser EE, Jones VJ, Tobias FA, Mackay AW (2017) Algal richness and life-history strategies are influenced by hydrology and phosphorus in two major subtropical wetlands. Freshw Biol 62(2):274–290. https://doi.org/10.1111/fwb.12866

McKee TB, Doesken NJ, Kleist J (1993) The relationship of drought frequency and duration to time scales, Paper Presented at 8th Conference on Applied Climatology. American Meteorological Society, Anaheim, CA, 17(22):179–183

Mendelsohn JM (2019) Landscape changes in Angola. In: Huntley BJ, Russo V, Lages F, Ferrand N (eds) Biodiversity of Angola. Science and conservation: a modern synthesis. Springer Nature, Cham, pp 123–137

Midgley GF, Thuiller W (2011) Potential responses of terrestrial biodiversity in Southern Africa to anthropogenic climate change. Reg Environ Change 11(1):127–135. https://doi.org/10.1007/s10113-010-0191-8

Mishra AK, Singh VP (2010) A review of drought concepts. J Hydrol 391(1–2):202–216. https://doi.org/10.1016/j.jhydrol.2010.07.012

Mlenga DH, Jordaan AJ, Mandebvu B (2019) Integrating standard precipitation index and normalised difference vegetation index for near-real-time drought monitoring in Eswatini. Jàmbá J Disaster Risk Stud 11(1):1–9. https://doi.org/10.4102/jamba.v11i1.917

Moreira EE, Coelho CA, Paulo AA, Pereira LS, Mexia JT (2008) SPI-based drought category prediction using loglinear models. J Hydrol 354(1–4):116–130. https://doi.org/10.1016/j.jhydrol.2008.03.002

Mulenga H (1999) Southern African climatic anomalies, summer rainfall and the Angola low. Ph.D. thesis, University of Cape Town, p 261

Nath R, Nath D, Li Q, Chen W, Cui X (2017) Impact of drought on agriculture in the Indo-Gangetic Plain. India Adv Atmos Sci 34(3):335–346. https://doi.org/10.1007/s00376-016-6102-2

Nhamo L, Mabhaudhi T, Modi AT (2019) Preparedness or repeated short-term relief aid? Building drought resilience through early warning in southern Africa. Water SA 45(1):75–85. https://doi.org/10.4314/wsa.v45i1.09

NOAA (2022) Cold & Warm Episodes by Season. https://origin.cpc.ncep.noaa.gov/products/analysis_monitoring/ensostuff/ONI_v5.php. Accessed 15 Jan 2022

NOAA (2021) El Niño/Southern Oscillation (ENSO). Southern Oscillation Index (SOI). https://www.ncdc.noaa.gov/teleconnections/enso/soi. Accessed 20 Nov 2021

Palmer WC (1965) Meteorological drought, vol 30. US Department of Commerce, Weather Bureau, Washington, DC

Palmer WC (1968) Keeping track of crop moisture conditions, nationwide: the new crop moisture index. Weatherwise 21(4):156–161. https://doi.org/10.1080/00431672.1968.9932814

Quammen D (2017) The mission to save Africa's Okavango Delta. Natl Geogr pp 80–103. https://www.nationalgeographic.com/magazine/article/africa-expedition-conservation-okavango-delta-cuito. Accessed 20 Sep 2021

Reason CJC, Jagadheesha D (2005) A model investigation of recent ENSO impacts over southern Africa. Meteorol Atmos Phys 89(1):181–205. https://doi.org/10.1007/s00703-005-0128-9

Reason CJC, Keibel A (2004) Tropical cyclone Eline and its unusual penetration and impacts over the southern African mainland. Weather Forecast 19(5):789–805. https://doi.org/10.1175/1520-0434(2004)019%3C0789:TCEAIU%3E2.0.CO;2

Regional Vulnerability Assessment and Analysis Programme (RVAA) (2019) Angola Vulnerability Assessment Committee Results 2019. https://reliefweb.int/sites/reliefweb.int/files/resources/SADC_Angola_snapshot_July2019.pdf Accessed 14 September 2021.

Rouault M, Richard Y (2005) Intensity and spatial extent of droughts in southern Africa. Geophys Res Lett 32(15):L15702. https://doi.org/10.1029/2005GL022436

Rouault M, Florenchie P, Fauchereau N and Reason CJC (2003) South East tropical Atlantic warm events and southern African rainfall. Geophysical Research Letters 30(5). https://doi.org/10.1029/2002GL014840

Rouse JW, Haas RH, Schell JA, Deering DW (1974) Monitoring vegetation systems in the Great Plains with ERTS. NASA Spec Publ 351:309

Svoboda M, Hayes M, Wood D (2012) Standardized precipitation index user guide (WMO-No. 1090), Geneva: World Meteorological Organization, p 25. https://digitalcommons.unl.edu/cgi/viewcontent.cgi?article=1208&context=droughtfacpub

Taylor PJ, Neef G, Keith M, Weier S, Monadjem A and Parker DM (2018) Tapping into technology and the biodiversity informatics revolution: updated terrestrial mammal list of Angola, with new records from the Okavango Basin. ZooKeys (779):51–88. https://zookeys.pensoft.net/article/25964/

Thomson MC, Abayomi K, Barnston AG, Levy M, Dilley M (2003) El Niño and drought in southern Africa. The Lancet 361(9355):437–438. https://doi.org/10.1016/S0140-6736(03)12421-X

Tirivarombo S, Osupile D, Eliasson P (2018) Drought monitoring and analysis: standardised precipitation evapotranspiration index (SPEI) and standardised precipitation index (SPI). Phys Chem Earth 106:1–10. https://doi.org/10.1016/j.pce.2018.07.001

Todd M, Washington R (1999) Circulation anomalies associated with tropical-temperate troughs in southern Africa and the south west Indian Ocean. Clim Dyn 15(12):937–951. https://doi.org/10.1007/s003820050323

Tsakiris G, Vangelis H (2005) Establishing a drought index incorporating evapotranspiration. Eur Water 9(10):3–11

United Nations Educational Scientific and Cultural Organization (UNESCO) (2021) World heritage List- Okavango. https://whc.unesco.org/en/list/1432/. Accessed 27 Nov 2021

United States Geological Survey (USGS) (2021). Landsat Surface Reflectance product overview. Available at https://www.usgs.gov/core-science-systems/nli/landsat/landsat-surface-reflectance?qtscience_support_page_related_con=0#qtcience_support_page_related_con. Accessed 20 September 2021.

Vicente-Serrano SM, Beguería S, López-Moreno JI (2010) A multiscalar drought index sensitive to global warming: the standardized precipitation evapotranspiration index. J Clim 23(7):1696–1718. https://doi.org/10.1175/2009JCLI2909.1

World Health Organisation (WHO) (2021) Drought overview. https://www.who.int/health-topics/drought#tab=tab_1. Accessed 15 September 2021.

World Wildlife Fund (WWF) (2021) Miombo woodlands facts and figures. https://wwf.panda.org/discover/knowledge_hub/where_we_work/miombo_woodlands/ Accessed 10 October 2021.

Yurco K, King B, Young KR, Crews KA (2017) Human–wildlife interactions and environmental dynamics in the Okavango Delta. Botsw Soc Nat Res 30(9):1112–1126. https://doi.org/10.1080/08941920.2017.1315655

Zargar A, Sadiq R, Naser B, Khan FI (2011) A review of drought indices. Environ Rev 19:333–349. https://doi.org/10.1139/a11-013